



CO₂ Absorption by DBU-Based Protic Ionic Liquids: Basicity of Anion Dictates the Absorption Capacity and Mechanism

Feixiang Gao^{1†}, Zhen Wang^{2†}, Pengju Ji^{1*} and Jin-Pei Cheng^{1,3*}

¹ Department of Chemistry, Center of Basic Molecular Science, Tsinghua University, Beijing, China, ² School of Chemical and Environmental Engineering, Anyang Institute of Technology, Anyang, China, ³ State Key Laboratory of Elemento-Organic Chemistry, Collaborative Innovation Center of Chemical Science and Engineering, Nankai University, Tianjin, China

OPEN ACCESS

Edited by:

Jason B. Harper,
University of New South Wales,
Australia

Reviewed by:

Tamar L. Greaves,
RMIT University, Australia
Ekaterina Pas,
Monash University, Australia

*Correspondence:

Pengju Ji
jipengju@mail.tsinghua.edu.cn
Jin-Pei Cheng
jinpei_cheng@mail.tsinghua.edu.cn

[†]These authors have contributed
equally to this work

Specialty section:

This article was submitted to
Green and Sustainable Chemistry,
a section of the journal
Frontiers in Chemistry

Received: 18 September 2018

Accepted: 18 December 2018

Published: 17 January 2019

Citation:

Gao F, Wang Z, Ji P and Cheng J-P
(2019) CO₂ Absorption by
DBU-Based Protic Ionic Liquids:
Basicity of Anion Dictates the
Absorption Capacity and Mechanism.
Front. Chem. 6:658.
doi: 10.3389/fchem.2018.00658

PILs are promising solvent systems for CO₂ absorption and transformations. Although previously tremendous work has been paid to synthesize functionalized PILs to achieve a high-performance absorption, the underlying mechanisms are far less investigated and still not clear. In this work, a series of DBU-based PILs, i.e., [DBUH][X], with anions of various basicities were synthesized. The basicities of the anions were accurately measured in [DBUH][OTf] or extrapolated from the known linear correlations. The apparent kinetics as well as the capacities for CO₂ absorption in these PILs were studied systematically. The results show that the absorption rate and capacity in [DBUH][X] are in proportional to the basicity of PIL, i.e., a more basic PIL leads to a faster absorption rate and a higher absorption capacity. In addition, the spectroscopic evidences and correlation analysis indicate that the capacity and mechanism of CO₂ absorption in [DBUH][X] are essentially dictated by the basicities of anions of these PILs.

Keywords: protic ionic liquids, basicity, CO₂ absorption, linear correlation, absorption mechanism and capacity

INTRODUCTION

Being considered as one of the major long-lived greenhouse gases that is responsible for the ever-increasing global warming phenomenon as well as ocean acidification (Jenkinson et al., 1999; Joos et al., 1999), carbon dioxide (CO₂) has triggered tremendous research efforts in both academic and industry (Benson et al., 2009; Aresta et al., 2014; Goepfert et al., 2014; Sanna et al., 2014; Xia et al., 2018). To date a plethora of research attentions have been given to the processing, utilization and recycling of CO₂, and one of the most fundamental research area among these studies is to design high-performance materials and develop a number of practical and efficient processes for CO₂ capture and storage (CCS) (Haszeldine, 2009; Boot-Handford et al., 2014). Traditional chemical absorption of CO₂ by aqueous solution of amines is a well-established process in this regard, and currently is an indispensable technology because of its low cost and good reactivity (Rao and Rubin, 2002). However, there have been growing concerns on the environmental issues associated with the use of aqueous amine solutions for CO₂ absorption, such as high volatility and corrosive nature, etc. In addition, the degradation of amines during the absorption is also well-known, which significantly impairs the absorption capacity (Gouedard et al., 2012). Thus, discovering eco-friendly solvents/solvent systems or designing advanced materials as a potential replacement for the traditional CO₂ absorption is highly desirable.

Ionic liquids (ILs) are composed of entirely ions and exhibit a number of properties that are significantly different from those of conventional molecular solvents. In addition, the cations and anions of ILs can be varied or functionalized, which may endow them with one or several favorable properties, such as negligible vapor pressure, low flammability, high conductivity, and good thermal stability (Welton, 1999; Hallett and Welton, 2011). As an important subset of ILs, protic ILs (PILs) can be conveniently prepared from stoichiometric neutralization between Brønsted acids and bases. Due to the presence of dissociable proton(s), compared with aprotic ILs (AILs), PILs exhibit a stronger hydrogen bond donicity and higher ionic conductivity under neat condition (Greaves and Drummond, 2008, 2015). Due to these merits that are distinctive from those of molecular solvents, ILs are labeled as green solvents (Rogers and Seddon, 2003) and have been extensively applied to catalysis, material and biological science as well as energy storage, etc. (van Rantwijk and Sheldon, 2007; Bideau et al., 2011; Watanabe et al., 2017).

Since Brennecke and co-worker demonstrated that CO₂ has a good solubility in an imidazolium-based room temperature IL in 1999 (Blanchard et al., 1999), tremendous research efforts has been paid to utilize ILs or functionalized-ILs as media for physical and chemical CO₂ absorptions during the past decades (Bates et al., 2002; Gurkan et al., 2010; Luo et al., 2014; Xia et al., 2018). These pioneer explorations on the CO₂ absorptions in various ILs suggest that the absorption capacity and enthalpy are closely associated with the identity and structure of comprising cation and anion (Wang et al., 2010, 2012). By varying the structure of anions for these protic ILs, equimolar or even more than equimolar CO₂ absorption has been achieved (Wang et al., 2011; Chen et al., 2016). Although a high absorption capacity of CO₂ has been realized in ILs, the fundamental rules that govern the absorption mechanism and performances are still not clear, which may hamper a rational design and development of ILs in this respect. In addition, currently the rationales for the catalytic performance of PILs on CO₂ absorption were almost entirely based on the acidity data determined in molecular solvents, such as water or DMSO (Wang et al., 2010; Yang et al., 2016). It is known from both experimental results and theoretical calculations that the acidity obtained in molecular solvents may not explain acid/base behavior in ILs satisfactorily (Mihichuk et al., 2011). For example, the absorption capacity of phosphonium-based ILs, i.e., [R₄P][X] (R = alkyl), was found sigmoidally (Yasuda and Watanabe, 2013) or linearly (Wang et al., 2012) correlated with the basicity of anion in molecular solvents. Therefore, it is sensible to use the acidity data determined in the ILs to assess CO₂ absorption capacity, which may shed some lights on the intrinsic ability of ILs for CO₂ absorption.

Superbase DBU-derived PILs [DBU = 1,5-diazabicyclo[5.4.0]-5-undecene] are promising solvent systems for the CO₂ absorption, previous studies have shown that CO₂ has a considerable solubility in these PILs (Losetty et al., 2017; Zhu et al., 2017). In this work, in order to systematically investigate the relationship between the absorption capacity and thermodynamic properties of ILs, firstly we synthesized

11 DBU-based PILs, i.e., [DBUH][X], whose anions (X⁻) are of different basicities (Figure 1), then the acidities of conjugated acids (HX) of these anions were determined or extrapolated from the known correlations obtained from previous study (Wang et al., 2018a). Next the apparent kinetics as well as capacity for CO₂ absorption in [DBUH][X] were measured, whereby the relationship between the basicity of anion X⁻ and CO₂ capture abilities of [DBUH][X] was established.

RESULTS AND DISCUSSION

Basicity Scale for the Anion (X⁻) in [DBUH][X] (Figure 1)

In our previous work, we have successfully measured the acidities for several series of commonly seen organic acids in a DBU-based PIL, i.e., [DBUH][OTf] (OTf⁻ = triflate) (Wang et al., 2018a). The regression analyses show that the acidities of structural and electronic different organic substrates, i.e., RO-H, N-H, N⁺-H, and RCOO-H, linearly correlate with those in water. However, instead of forming a unified straight line, which is the case found for the analogous acidity correlation between a PIL EAN (ethylammonium nitrate) and water (Kanzaki et al., 2016), each individual series exhibits different slope and intercept (Figure 2) (Wang et al., 2018a). These linear acidity correlations between PILs and molecular solvent water are highly useful for accessing pK_a values of compounds in neat PILs that are difficult to determine due to the solvent leveling effect.

$$\text{For } \text{N}^+ - \text{H acids: } \text{p}K_{\text{a}}^{[\text{DBUH}][\text{OTf}]} = 1.07\text{p}K_{\text{a}}^{\text{water}} + 2.60 \quad (1)$$

$$\text{For } \text{N} - \text{H acids: } \text{p}K_{\text{a}}^{[\text{DBUH}][\text{OTf}]} = 0.775\text{p}K_{\text{a}}^{\text{water}} + 6.93 \quad (2)$$

$$\text{For } \text{O} - \text{H acids: } \text{p}K_{\text{a}}^{[\text{DBUH}][\text{OTf}]} = 1.28\text{p}K_{\text{a}}^{\text{water}} + 3.78 \quad (3)$$

$$\text{For } \text{COO} - \text{H acids: } \text{p}K_{\text{a}}^{[\text{DBUH}][\text{OTf}]} = 1.34\text{p}K_{\text{a}}^{\text{water}} + 5.26 \quad (4)$$

As shown in Figure 2, from the linear correlation of N⁺-H series, the acidity of protonated DBU, i.e., DBUH⁺ can be extrapolated as pK_a = 15.1 in neat [DBUH][OTf]¹, which suggests that the acidities of these substrates with a pK_a close to and above this value (> ~14) are very difficult to be measured in neat [DBUH][OTf] by classical UV-vis spectroscopic approach (Yang et al., 2018). However, with the correlation equations provided in Figure 2, the basicities of a series of strong basic anions (1–8, Figure 1) for [DBUH][X] can be conveniently extrapolated from the linear correlation equations (Equations 1–4). Together with 3 experimentally determined basicities of less basic anions (9–11, Figure 1), a basicity scale that comprises totally 11 basicity values of anions (as expressed by the acidities of their anion precursors HX) involved in this work was established. Although

¹From the correlation equation for N⁺-H series (Figure 2), the autoprotolysis constant of [DBUH][OTf], $\text{p}K_{\text{auto}}^{[\text{DBUH}][\text{OTf}]} = [\text{DBU}][\text{HOTf}] = 14.5$ can also be derived as follow: $K_{\text{a}} = [\text{DBU}][\text{H}^+]/[\text{DBUH}^+] = K_{\text{auto}}^{[\text{DBUH}][\text{OTf}]} / [\text{DBUH}^+]$, therefore: $K_{\text{auto}}^{[\text{DBUH}][\text{OTf}]} = [\text{DBUH}^+] \cdot K_{\text{a}}$, the molar concentration of [DBUH][OTf] at 25 °C (4.45 mol/L) can be calculated from the density [1.345 g/cm³ at 25°C (Miran et al., 2012)] and molecular weight (302.3 g/mol) of [DBUH][OTf]. $\text{p}K_{\text{auto}}^{[\text{DBUH}][\text{OTf}]}$ is about 0.5 or 4.5 pK units higher than that of water or EAN [$\text{p}K_{\text{auto}}^{\text{EAN}} = 10.0$ (Kanzaki et al., 2016)], respectively.

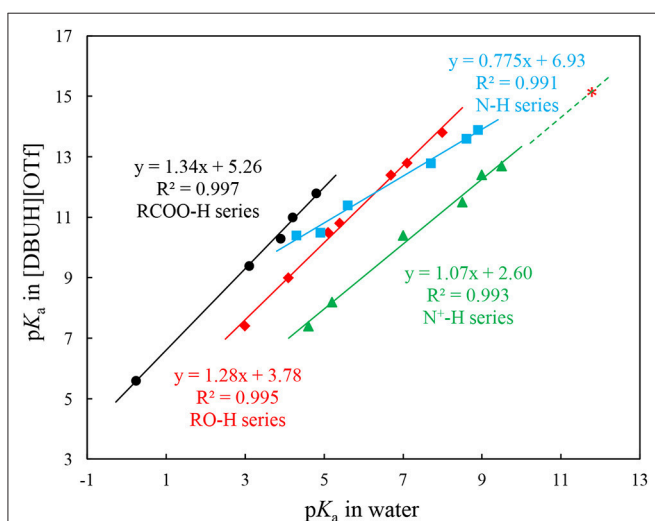
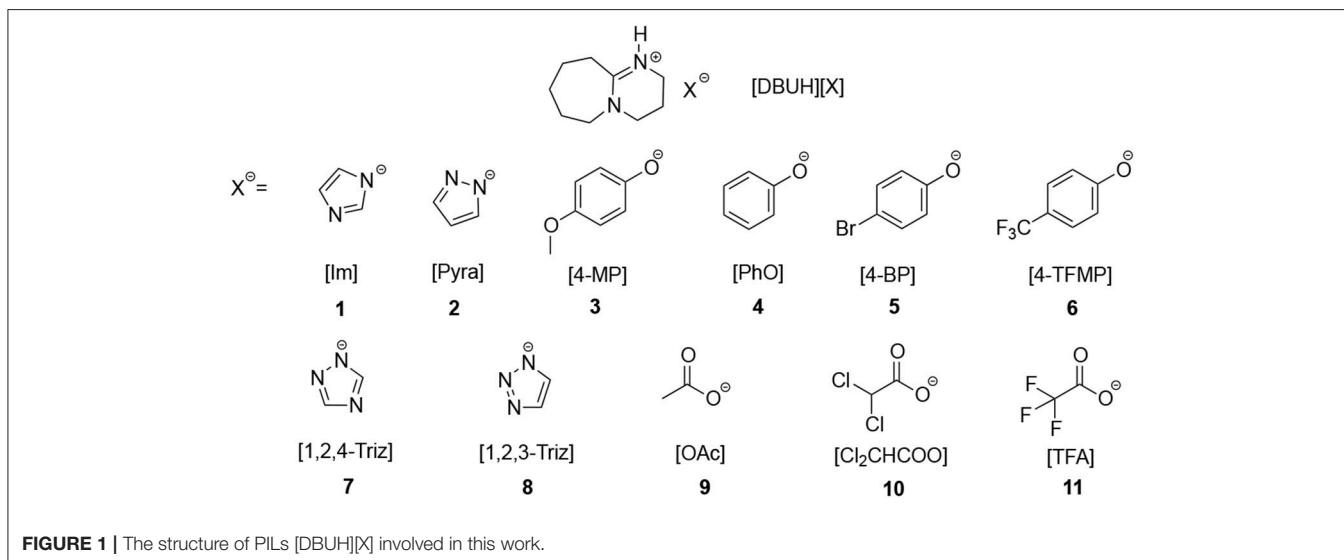


FIGURE 2 | Correlations between pK_a s of N-H (■), N-H⁺ (▲), RO-H (◆), and carboxylic (RCOO-H, ●) acids in [DBUH][OTf] and those in water. The red asterisk (*) shows the extrapolated pK_a value of 15.1 for DBUH⁺ [$pK_a^{\text{DBUH}^+}$ in water = 11.7, (Kaupmees et al., 2014)] in [DBUH][OTf] from the linear correlation of N⁺-H series (Equation 1)¹. Equations 1–4 were obtained from these linear correlations in **Figure 2** and used to extrapolate the pK_a s of anion precursors HX (1–8, **Table 1**) in [DBUH][OTf] (**Table 1**), in specific, the pK_a s of 1, 2, 7, and 8 are from Equation 2 and those of 3–6 are from Equation 3.

these basicity values were acquired in [DBUH][OTf] and may be different from those in the PILs [DBUH][X], the relative basicity and nucleophilicity order of these anions are expected to be consistent between the DBU-based PILs. **Table 1** lists the acidity of anion precursor (HX) in [DBUH][OTf], together with those available data in molecular solvents. As shown in **Table 1**, the basicity scale for the anions of [DBUH][X] covers 13 pK units and the basicities of these anions in [DBUH][OTf] are similar to those in DMSO but significantly greater than in water.

CO₂ Absorption in [DBUH][X]

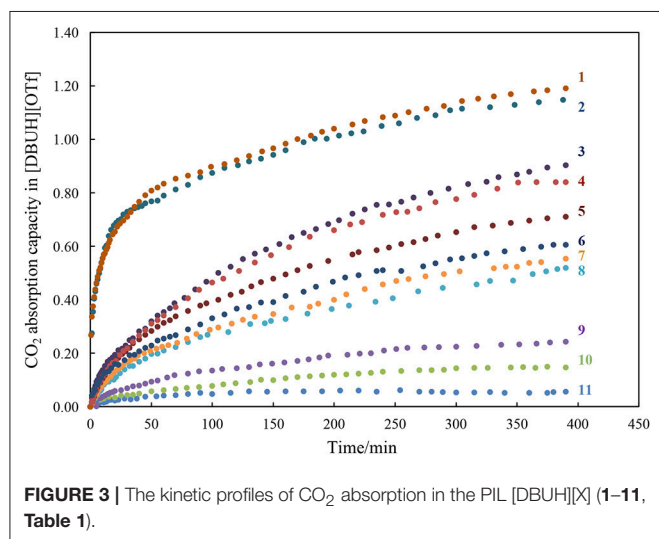
With the basicity scale for the anions in our hands, next we systematically measured the apparent kinetic of CO₂ absorption in [DBUH][X], with a control of temperature at constant 25°C by a thermostat and the measurement was performed under atmosphere pressure. The CO₂ absorption capacity in the individual [DBUH][X] is also determined as the molar ratio between the maximum amount of CO₂ absorbed and of [DBUH][X] used (**Table 1**). It is worth noting that the viscosity of [DBUH][X] increased with the increasing amount of CO₂ absorbed, forming a gel-like liquid which leads to a relatively large standard deviation (SD = ±0.05 of the absorption molar ratio). However, the volume of PILs did not have an obvious increase through CO₂ uptake, which is in line with the previous reported (Firaha and Kirchner, 2014). **Figure 3** shows the apparent kinetic profile of CO₂ absorption in these PILs, in general, the rates for CO₂ absorption in [DBUH][X] are slower than those observed in phosphonium-based aprotic ILs ([PR₄][X]), probably due to the hydrogen bonding between DBUH⁺ and X⁻ in [DBUH][X], which makes anions less reactive toward CO₂ than those in [PR₄][X] (Wang et al., 2011). As also can be seen from **Figure 3**, the rate of CO₂ absorption is faster in the [DBUH][X] with a more basic anion X⁻ than in those with less basic ones. In addition, as shown from **Table 1**, the maximum absorption capacity of [DBUH][X] decreases with the decreasing basicity of anions. For examples, the amount of CO₂ uptake for the most basic [DBUH][Im] (1) is about twice as much as that for the less basic [DBUH][4-TFMP] (6). On the other hand, there is a sharp decrease in CO₂ absorption capacity in these weakly basic PILs (8–11), as for the least basic PILs, such as [DBUH][TFA] (11) and [DBUH][Cl₂CHCOO] (10), they both have a very limited absorption ability, despite of their obvious basicity difference.

In order to understand the absorption mechanism, the CO₂ absorption in [DBUH][X] was monitored by NMR and IR spectroscopies. The ¹³C NMR and IR spectra for

TABLE 1 | The acidity of anion precursor (HX) in [DBUH][OTf] and the corresponding CO₂ absorption capacity in [DBUH][X].

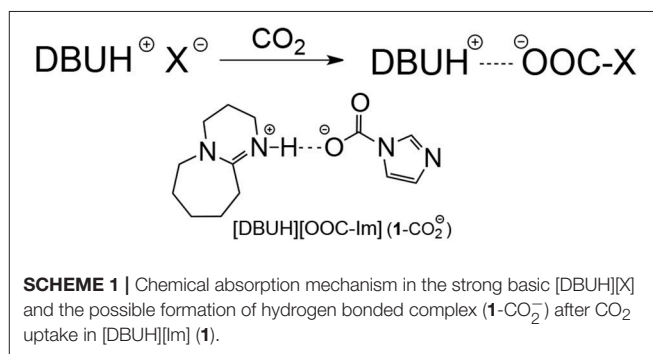
Entry	[DBUH][X]	^a pK _a [DBUH][OTf] (HX)	^{a,b} pK _a water (HX)	^{a,b} pK _a DMSO (HX)	CO ₂ absorption ^c
1	[DBUH][Im]	18.2 ^d	14.5	18.6	1.19
2	[DBUH][Pyr]	17.7 ^d	13.9	19.8	1.15
3	[DBUH][4-MP]	16.8 ^d	10.2	19.1	0.90
4	[DBUH][PhO]	16.6 ^d	10.0	18.0	0.84
5	[DBUH][4-BP]	15.8 ^d	9.4	16.4	0.70
6	[DBUH][4-TFMP]	14.9 ^d	8.7	15.2	0.61
7	[DBUH][1,2,4-Triz]	14.7 ^d	10.0	14.7 ₅	0.55
8	[DBUH][1,2,3-Triz]	14.3 ^d	9.5	13.9	0.52
9	[DBUH][OAc]	11.8 ^e	4.7 ₅	12.5	0.24
10	[DBUH][Cl ₂ CHCOO]	7.6 ^e	1.3 ₅	6.4	0.06
11	[DBUH][TFA]	5.6 ^e	0.23	3.6	0.05

^aThe conjugated acid HX of the corresponding anion in [DBUH][X]. ^bpK_a data is from: Internet Bond-energy Databank (iBond), ibond.chem.tsinghua.edu.cn or ibond.nankai.edu.cn. ^cMol CO₂ per mol PIL, the experiments were conducted at constant 25°C under atmospheric pressure, SD = ± 0.05, which is based on 3 individual absorption experiments. ^dExtrapolated values obtained from the corresponding linear correlations (Figure 2 and Equations 1–4). ^eDetermined experimentally, SD ≤ ± 0.05 pK units.

**FIGURE 3** | The kinetic profiles of CO₂ absorption in the PIL [DBUH][X] (1–11, Table 1).

each [DBUH][X] before and after CO₂ absorption were recorded and compared (Supplementary Material provides full characterizations, herein only a representative example is presented). Spectroscopic results show that there is no change in both ¹³C NMR and IR spectra before and after the absorption for [DBUH][X] with a relatively weak basic anion (8–11, Table 1, for details, see Supplementary Material). Presumably, this is due to the basicities of anions for these PILs are too weak to react with CO₂ to form the corresponding carboxylates (Scheme 1, vide infra), therefore a physical absorption mechanism likely dominates in these PILs (Izgorodina et al., 2015).

By contrast, the [DBUH][X] with relatively strong basic anions (1–7, Figure 1) clearly exhibit a different absorption mechanism as revealed by the results from ¹³C NMR and IR spectra. Compared with those before CO₂ uptake, the IR and ¹³C NMR spectra of 1–7 after CO₂ uptake show a new peak at ~1,700 cm⁻¹ (C=O stretching) and a new signal at ~163 ppm



which are characteristic of carbonyl carbons in carbamates or carbonates, respectively (Figures 4, 5, Supplementary Material). As a representative example, the IR spectrum of [DBUH][Im] (1) after absorption shows a distinctive peak at 1,696 cm⁻¹, in addition, a new signal at 161.5 ppm was observed in ¹³C NMR spectrum (Figures 4, 5).

These spectra results indicate that the mechanism for [DBUH][X] with a relatively strong basic anion (1–7) follows a chemical absorption mechanism (Wang et al., 2011; Chen et al., 2016). As illustrated in Scheme 1, the anions of 1–7 react with CO₂ through a nucleophilic attack process which yields the corresponding carboxylate adducts [DBUH][OOC-X], and the rate of forming carboxylate is in proportion to the basicity of anion which, under most circumstances, is paralleled with its nucleophilicity (Figure 3)².

Linear correlation can be a useful tool to reveal the underlying factors that govern the absorption kinetic and mechanism. In this connection, the correlation between the absorption capacity

²Although in some cases, there do exist discrepancies between nucleophilicity and basicity of nucleophile and the traditional Brønsted analysis fails (Mayr and Ofial, 2016). However, recent studies show that linear correlations were found between basicity and nucleophilicity of N-heterocyclic carbenes (NHCs) in the reactions that involving CO₂ as the substrate (Niu et al., 2017; Wang et al., 2018,b).

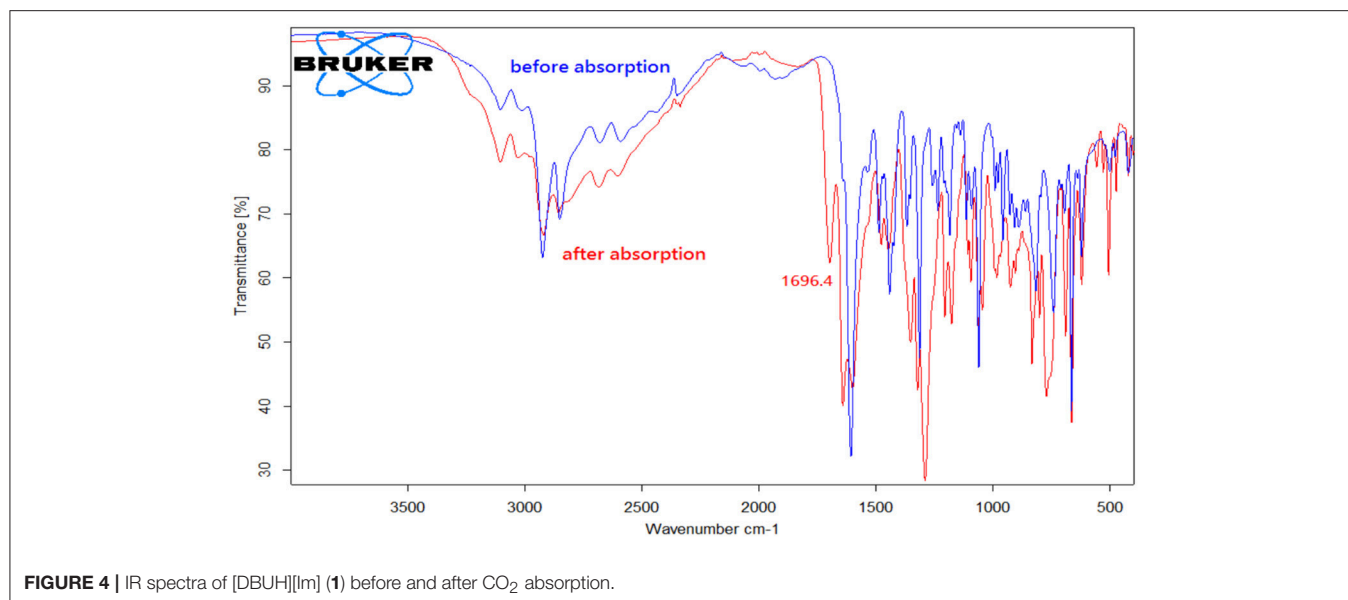


FIGURE 4 | IR spectra of [DBUH][Im] (**1**) before and after CO₂ absorption.

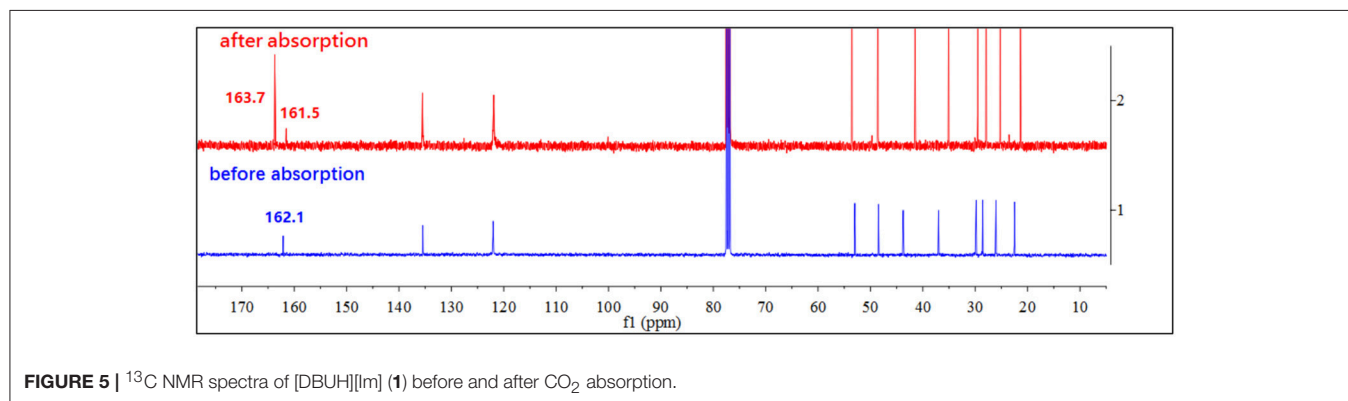


FIGURE 5 | ¹³C NMR spectra of [DBUH][Im] (**1**) before and after CO₂ absorption.

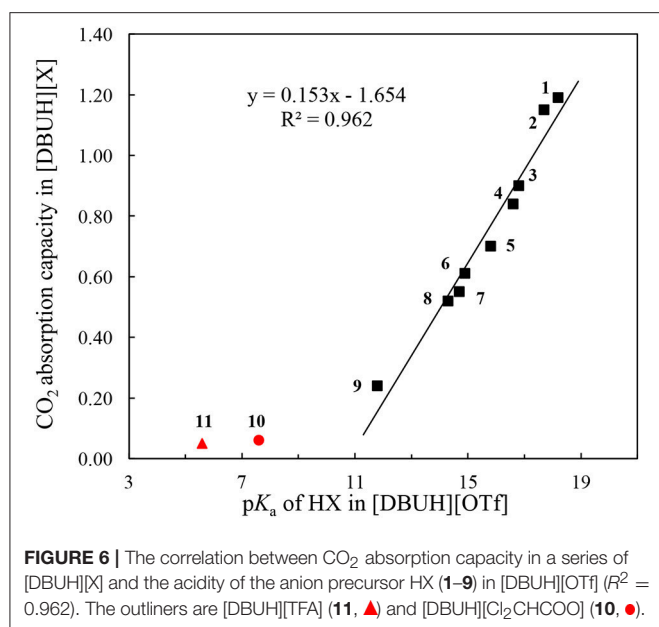
of [DBUH][X] and the basicity of anion in [DBUH][OTf] was performed. As shown in **Figure 6**, one can clearly notice a transition of CO₂ absorption capacity which is regulated by the basicity of anion. Specifically, there is a fairly good linear relationship ($R^2 = 0.962$) between the absorption capacity in [DBUH][X] (**1–9**) and the basicity of anion in [DBUH][OTf], excluding the data points of very weakly basic [DBUH][TFA] (**11**) and [DBUH][Cl₂CHCOO] (**10**). Combined with the evidences from the spectroscopic studies, we can conclude with confidence that a chemical absorption mechanism occurs in the [DBUH][X] (**1–7**) whose anion precursor HX has a $pK_a > 15$ in [DBUH][OTf], while the CO₂ absorption follows a physical absorption mechanism in [DBUH][X] (**10–11**) with an anion precursor's $pK_a < 10$. Presumably, a mixed chemical and physical mechanism occurs in these PILs with an anion precursor pK_a between 10 and 15, such as the CO₂ absorption in **8** and **9**. The quantum chemical calculations would be an ideal tool for the mechanism elucidation of CO₂ absorption in the PILs, however, currently some crucial physical and chemical parameters, such as dielectric constants, etc., for these PILs [DBUH][X] are not yet available, which hampers a detailed

and reliable theoretical calculation for the CO₂ absorption mechanism study in these PILs. It is worth noting that, by contrast, a similar correlation between absorption capacity and pK_a for precursor (**1–9**) of anion in molecular solvents, such as water and DMSO exhibits an inferior linear correlation ($R^2 = 0.874$ and 0.898 , respectively, **Figures S36, S37**), which implies that the bond energetic data obtained in molecular solvents, though relatively abundant and well-established, may not be suitable to interpret the experimental observations in ILs. Therefore, cares should be taken when one attempts to utilize the thermodynamic parameters measured in *molecular solvents* to disclose the governing factors for the gas absorptions in *PILs*.

EXPERIMENTAL

Chemicals and CO₂ Gas

All the chemicals and solvents were purchased from commercially available sources, and used directly without further purification except otherwise noted. DBU was also from commercially available sources, but purified from multiple reduced pressure distillation. CO₂ gas was provided by the Linde



Industrial Gases with a purity of >99.9995%, and was directly generated into [DBUH][X] for the CO₂ absorption.

Instrumentations

The IR spectra were recorded on a Bruker Tensor II FT-IR instrument. The ¹H NMR and ¹³C NMR spectra were recorded on a Bruker AVANCE III HD 400 MHz spectrometer. The water content was determined by a Mettler Toledo V20S compact volumetric Karl-Fischer titrator. UV-vis spectra were obtained from an Agilent Cary 100 machine with the control of temperature at constant 25°C.

Preparation of [DBUH][X]

[DBUH][X] were synthesized by direct equal molar neutralization reactions between DBU and acids under neat condition or in methanol, **Supplementary Material** provides the detailed synthetic procedures. The structure of [DBUH][X] were confirmed by NMR and IR spectroscopies. The water content of prepared [DBUH][X] varies from 100 to 300 ppm, which was determined by a Karl-Fisher titration machine. It is worth noting that the water content of [DBUH][X] has only a limited effect on the CO₂ absorption in the range of 100 to 300 ppm, as the comparison experiments showed that nearly the identical amount of CO₂ was absorbed by the [DBUH][X] with a water content of 100 or 300 ppm.

[DBUH][Im] (1): ¹H NMR (400 MHz, CDCl₃) δ 11.49 (br, 1H), 7.64 (s, 1H), 7.06 (s, 2H), 3.57–2.96 (m, 6H), 2.39 (s, 2H), 1.90–1.74 (m, 2H), 1.72–1.32 (m, 6H); ¹³C NMR (101 MHz, CDCl₃) δ 162.1, 135.5, 122.0, 53.0, 48.5, 43.7, 37.0, 29.8, 28.6, 26.0, 22.5 ppm; IR (neat): 3147, 2923, 2850, 2779, 2742, 2671, 2349, 1999, 1608 cm⁻¹;

[DBUH][Pyra] (2): ¹H NMR (400 MHz, CDCl₃) δ 12.63 (br, 0.49H), 7.53 (d, *J* = 1.8 Hz, 2H), 6.24 (t, *J* = 1.8 Hz, 1H), 3.26

(t, *J* = 5.5 Hz, 2H), 3.20–3.08 (m, 4H), 2.42–2.26 (m, 2H), 1.82–1.70 (m, 2H), 1.68–1.41 (m, 6H); ¹³C NMR (101 MHz, CDCl₃) δ 162.1, 133.3, 104.3, 52.9, 48.4, 43.5, 36.8, 29.7, 28.4, 25.8, 22.3 ppm; IR (neat): 3142, 3049, 2924, 2850, 2675, 2350, 1900, 1607 cm⁻¹;

[DBUH][4-MP] (3): ¹H NMR (400 MHz, CDCl₃) δ 12.35 (br, 0.74H), 6.76–6.64 (m, 4H), 3.69 (s, 3H), 3.29–3.16 (m, 6H), 2.50–2.40 (m, 2H), 1.84–1.74 (m, 2H), 1.66–1.49 (m, 6H); ¹³C NMR (101 MHz, CDCl₃) δ 163.0, 154.1, 151.5, 116.8, 114.7, 55.9, 53.1, 48.4, 42.0, 35.1, 29.6, 28.1, 25.5, 21.8 ppm; IR (neat): 2926, 2852, 2666, 2510, 2349, 2109, 1606 cm⁻¹;

[DBUH][PhO] (4): ¹H NMR (400 MHz, CDCl₃) δ 13.26 (br, 0.85H), 7.18–7.05 (m, 2H), 6.88–6.75 (m, 2H), 6.66 (t, *J* = 7.3 Hz, 1H), 3.31–3.25 (m, 2H), 3.23 (t, *J* = 6.2 Hz, 4H), 2.56–2.37 (m, 2H), 1.89–1.75 (m, 2H), 1.72–1.47 (m, 6H). ¹³C NMR (101 MHz, CDCl₃) δ 163.2, 160.8, 129.3, 117.0, 116.7, 53.2, 48.4, 41.8, 35.0, 29.6, 28.1, 25.4, 21.7 ppm; IR (neat): 3047, 2925, 2852, 2684, 2455, 2349, 2094, 1816, 1581 cm⁻¹;

[DBUH][4-BP] (5): ¹H NMR (400 MHz, CDCl₃) δ 7.09 (d, *J* = 8.7 Hz, 2H), 6.67–6.56 (m, 2H), 3.24 (dd, *J* = 12.4, 6.9 Hz, 6H), 2.61–2.48 (m, 2H), 1.88–1.74 (m, 2H), 1.68–1.45 (m, 6H); ¹³C NMR (101 MHz, CDCl₃) δ 164.7, 161.3, 131.8, 118.9, 107.4, 53.7, 48.4, 39.6, 33.3, 29.2, 27.3, 24.6, 20.4 ppm; IR (neat): 2926, 2853, 2449, 2349, 2101, 1860, 1640 cm⁻¹;

[DBUH][4-TFMP] (6): ¹H NMR (400 MHz, CDCl₃) δ 12.51 (br, 1H), 7.31 (d, *J* = 8.6 Hz, 2H), 6.72 (d, *J* = 8.6 Hz, 2H), 3.33–3.23 (m, 6H), 2.60–2.52 (m, 2H), 1.92–1.81 (m, 2H), 1.73–1.54 (m, 6H); ¹³C NMR (101 MHz, CDCl₃) δ 166.8, 164.3, 126.8 (q, *J*_{C-F} = 3.7 Hz), 125.6 (q, *J* = 270.0 Hz), 117.2, 116.8 (q, *J*_{C-F} = 32.1 Hz), 53.6, 48.5, 40.5, 33.9, 29.4, 27.7, 25.0, 21.0 ppm; IR (neat): 2930, 2859, 2675, 2349, 2100, 1856, 1640, cm⁻¹;

[DBUH][1,2,4-Triz] (7): ¹H NMR (400 MHz, CDCl₃) δ 14.81 (br, 1H), 8.06 (s, 2H), 3.48–3.14 (m, 6H), 2.78–2.41 (m, 2H), 1.93–1.82 (m, 2H), 1.72–1.54 (m, 6H); ¹³C NMR (101 MHz, CDCl₃) δ 164.2, 148.3, 53.6, 48.5, 40.6, 34.2, 29.4, 27.7, 25.0, 21.0 ppm; IR (neat): 3078, 2925, 2855, 2473, 2350, 2072, 1898, 1638, 1611 cm⁻¹;

[DBUH][1,2,3-Triz] (8): ¹H NMR (400 MHz, CDCl₃) δ 12.60 (br, 1H), 7.59 (d, *J* = 19.6 Hz, 2H), 3.63–3.02 (m, 6H), 2.90–2.56 (m, 2H), 1.93–1.80 (m, 2H), 1.58 (dd, *J* = 25.3, 3.8 Hz, 6H); ¹³C NMR (101 MHz, CDCl₃) δ 165.1, 130.0, 53.8, 48.4, 39.1, 33.0, 29.1, 27.2, 24.4, 20.1 ppm; IR: 3234, 3101, 2926, 2857, 2672, 2117, 1881, 1637 cm⁻¹;

[DBUH][OAc] (9): ¹H NMR (400 MHz, CDCl₃) δ 3.46–3.26 (m, 6H), 2.81 (d, *J* = 5.4 Hz, 2H), 1.99–1.85 (m, 5H), 1.68 (m, 4H), 1.60 (m, 2H); ¹³C NMR (101 MHz, CDCl₃) δ 177.4, 165.6, 53.8, 48.3, 37.7, 31.6, 28.8, 26.8, 24.4, 23.9, 19.5 ppm; IR (neat): 3249, 2925, 2859, 2670, 2349, 2103, 1887, 1641, cm⁻¹;

[DBUH][Cl₂CHCOO] (10): ¹H NMR (400 MHz, CDCl₃) δ 11.76 (br, 1H), 5.80 (s, 1H), 3.60–3.18 (m, 6H), 2.76 (d, *J* = 6.0 Hz, 2H), 2.08–1.78 (m, 2H), 1.75–1.55 (m, 6H); ¹³C NMR (101 MHz, CDCl₃) δ 168.3, 166.2, 70.0, 54.4, 48.7, 38.3, 32.3, 29.1, 26.9, 24.2, 19.7 ppm; IR (neat): 3229, 2929, 2859, 2802, 1632, 1377 cm⁻¹;

[DBUH][TFA] (11): ¹H NMR (400 MHz, CDCl₃) δ 11.23 (br, 1H), 3.48–3.37 (m, 4H), 3.32 (dd, *J* = 7.8, 5.9 Hz, 2H), 2.79–2.65 (m, 2H), 2.00–1.89 (m, 2H), 1.63 (ddd, *J* = 14.7, 8.4, *J* = 5.4 Hz,

6H); ¹³C NMR (101 MHz, CDCl₃) δ: 166.2, 161.3, 117.1, 54.3, 48.5, 38.1, 32.2, 28.9, 26.7, 23.9, 19.4 ppm; IR (neat): 3232, 3101, 3042, 2933, 2864, 2813, 1687, 1640 cm⁻¹;

CO₂ Absorption in [DBUH][X]

The absorption capacity of CO₂ was measured according to the standard procedures reported (Wang et al., 2010, 2011). In specific, about 1.0 g [DBUH][X] was added to a 10 ml Schlenk tube which was pre-flushed with CO₂ gas. With agitation and control of temperature by a thermostat, a stream of CO₂ was bubbled into [DBUH][X] with a flow rate of 60 ml/min through a stainless steel needle (inner diameter = 10 mm) under atmosphere pressure. The weight of the tube was monitored from time to time until no further increment was detected by an electronic balance with an accuracy of ±0.1 mg. CO₂ absorption capacity in [DBUH][X] was then calculated based on the mass increasing of the Schlenk tube.

pK_a Determinations in [DBUH][OTf]

The UV-vis spectroscopic method was used the pK_a determination of the substrates involved in this work. The acidity ladder scale and indicator acids, the special UV cell and detailed procedures are similar to the previously reported (Wang et al., 2018a). The concentration of substrate acids was 10⁻⁴ to 10⁻³ M, the water content of [DBUH][OTf] was less than 100 ppm and the base used in the acidity determination in [DBUH][OTf] was DBU. The pK_a for each substrate was the average of 3 individual experiments, and the standard deviation (SD) is less than ±0.05 pK units.

CONCLUSIONS

In summary, we synthesized 11 DBU-based PILs with different basicity in [DBUH][OTf] and systematically investigated their CO₂ absorption kinetic and capacity in these PILs. The

basicity scale for the anion of these PILs in [DBUH][OTf] was established by extrapolation or direct determination. The CO₂ absorption in the weakly basic PILs are slow and practically have negligible absorption capacity, which is in line with a physical absorption mechanism. On the other hand, faster rates and higher absorption capacity were observed in the strongly basic PILs, and the spectroscopic studies support a chemical absorption mechanism in these PILs. The correlation between CO₂ absorption capacities and basicities of PILs, excluding those very weakly basic ones, in [DBUH][OTf] shows an excellent linear relationship, which indicates that the basicity of anion dictates the absorption ability and mechanism. We hope these results can be of help for a better understanding of structural implication of PILs on the CO₂ absorption, and also for a rational design of PILs in this connection.

AUTHOR CONTRIBUTIONS

PJ and J-PC conceived and designed the experiments and supervised the project; FG and ZW performed the experiments; FG, PJ, and J-PC prepared and revised the manuscript.

ACKNOWLEDGMENTS

This work is supported by the financial grants from National Natural Science Foundation of China (Nos. 21672124, 21390401), the partial of this work was also supported by Tsinghua University Initiative Scientific Research Program (No. 2015Z99003).

SUPPLEMENTARY MATERIAL

The Supplementary Material for this article can be found online at: <https://www.frontiersin.org/articles/10.3389/fchem.2018.00658/full#supplementary-material>

REFERENCES

- Aresta, M., Dibenedetto, A., and Angelini, A. (2014). Catalysis for the valorization of exhaust carbon: from CO₂ to chemicals, materials, and fuels. Technological use of CO₂. *Chem. Rev.* 114, 1709–1742. doi: 10.1021/cr4002758
- Bates, E. D., Mayton, R. D., Ntai, I., and Davis, J. H. (2002). CO₂ capture by a task-specific ionic liquid. *J. Am. Chem. Soc.* 124, 926–927. doi: 10.1021/ja017593d
- Benson, E. E., Kubiak, C. P., Sathrum, A. J., and Smieja, J. M. (2009). Electrocatalytic and homogeneous approaches to conversion of CO₂ to liquid fuels. *Chem. Soc. Rev.* 38, 89–99. doi: 10.1039/B804323J
- Bideau, J. L., Viau, L., and Vioux, A. (2011). Ionogels, ionic liquid based hybrid materials. *Chem. Soc. Rev.* 40, 907–925. doi: 10.1039/C0CS00059K
- Blanchard, L. A., Hancu, D., Beckman, E. J., and Brennecke, J. F. (1999). Green processing using ionic liquids and CO₂. *Nature* 399, 28–29. doi: 10.1038/19887
- Boot-Handford, M. E., Abanades, J. C., Anthony, E. J., Blunt, M. J., Brandani, S., MacDowell, N., et al. (2014). Carbon capture and storage update. *Energy Environ. Sci.* 7, 130–189. doi: 10.1039/C3EE42350F
- Chen, F. F., Huang, K., Zhou, Y., Tian, Z. Q., Zhu, X., Tao, D. J., et al. (2016). Multi-molar absorption of CO₂ by the activation of carboxylate groups in amino acid ionic liquids. *Angew. Chem. Int. Ed.* 55, 7166–7170. doi: 10.1002/anie.201602919
- Firaha, D. S., and Kirchner, B. (2014). CO₂ absorption in the protic ionic liquid ethylammonium nitrate. *J. Chem. Eng. Data* 59, 3098–3104. doi: 10.1021/je500166d
- Goeppert, A., Czaun, M., Jones, J., Surya Prakash, G. K., and Olah, G. A. (2014). Recycling of carbon dioxide to methanol and derived products—closing the loop. *Chem. Soc. Rev.* 43, 7995–8048. doi: 10.1039/C4CS00122B
- Gouedard, C., Picq, D., Launay, F., and Carrette, P. L. (2012). Amine degradation in CO₂ capture. I. A review. *Int. J. Greenh. Gas Con.* 10, 244–270. doi: 10.1016/j.ijggc.2012.06.015
- Greaves, T. L., and Drummond, C. J. (2008). Protic ionic liquids: Properties and applications. *Chem. Rev.* 108, 206–237. doi: 10.1021/cr068040u
- Greaves, T. L., and Drummond, C. J. (2015). Protic ionic liquids: Evolving structure–property relationships and expanding applications. *Chem. Rev.* 115, 11379–11448. doi: 10.1021/acs.chemrev.5b00158
- Gurkan, B. E., de la Fuente, J. C., Mindrup, E. M., Ficke, L. E., Goodrich, B. F., Price, E. A., et al. (2010). Equimolar CO₂ absorption by anion-functionalized ionic liquids. *J. Am. Chem. Soc.* 132, 2116–2117. doi: 10.1021/ja909305t
- Hallett, J. P., and Welton, T. (2011). Room-temperature ionic liquids. Solvents for synthesis and catalysis 2. *Chem. Rev.* 111, 3508–3576. doi: 10.1021/cr1003248
- Haszeldine, R. S. (2009). Carbon capture and storage: how green can black be? *Science* 325, 1647–1652. doi: 10.1126/science.1172246
- Izgorodina, E. I., Hodgson, J. L., Weis, D. C., Pas, S. J., and MacFarlane, D. R. (2015). Physical absorption of CO₂ in protic and aprotic ionic

- liquids: an interaction perspective. *J. Phys. Chem. B* 119, 11748–11759. doi: 10.1021/acs.jpcc.5b05115
- Jenkinson, D. S., Adams, D. E., and Wild, A. (1999). Model estimates of CO₂ emissions from soil in response to global warming. *Nature* 351, 304–306.
- Joos, F., Plattner, G. K., Stocker, T. F., Marchal, O., and Schmittner, A. (1999). Global warming and marine carbon cycle feedbacks on future atmospheric CO₂. *Science* 284, 464–467. doi: 10.1126/science.284.5413.464
- Kanzaki, R., Kodamatani, H., Tomiyasu, T., Watanabe, H., and Umeyayashi, Y. (2016). A pH scale for the protic ionic liquid ethylammonium nitrate. *Angew. Chem. Int. Ed.* 55, 6266–6269. doi: 10.1002/anie.201511328
- Kaupmees, K., Trummal, A., and Leito, I. (2014). Basicities of strong bases in water: a computational study. *Croat. Chem. Acta* 87, 385–395. doi: 10.5562/cca2472
- Losetty, V., Matheswaran, P., and Wilfred, C. D. (2017). Synthesis, thermophysical properties and COSMO-RS study of DBU based protic ionic liquids. *J. Chem. Thermodyn.* 105, 151–158. doi: 10.1016/j.jct.2016.10.021
- Luo, X. Y., Guo, Y., Ding, F., Zhao, H. Q., Cui, G. K., Li, H. R., et al. (2014). Significant improvements in CO₂ capture by pyridine-containing anion-functionalized ionic liquids through multiple-site cooperative interactions. *Angew. Chem. Int. Ed.* 53, 7053–7057. doi: 10.1002/anie.201400957
- Mayr, H., and Ofial, A. R. (2016). Philicities, fugacities, and equilibrium constants. *Acc. Chem. Res.* 49, 952–965. doi: 10.1021/acs.accounts.6b00071
- Mihichuk, L. M., Driver, G. W., and Johnson, K. E. (2011). Brønsted acidity and the medium: fundamentals with a focus on ionic liquids. *ChemPhysChem* 12, 1622–1632. doi: 10.1002/cphc.201100087
- Miran, M. S., Kinoshita, H., Yasuda, T., Md. Susan, A. B. H., and Watanabe, M. (2012). Physicochemical properties determined by ΔpK_a for protic ionic liquids based on an organic super-strong base with various Brønsted acids. *Phys. Chem. Chem. Phys.* 14, 5178–5186. doi: 10.1039/c2cp00007e
- Niu, Y., Wang, N., Muñoz, A., Xu, J., Zeng, H., Rovis, T., et al. (2017). Experimental and computational gas phase acidities of conjugate acids of triazolylidene carbenes: rationalizing subtle electronic effects. *J. Am. Chem. Soc.* 139, 14917–14930. doi: 10.1021/jacs.7b05229
- Rao, A. B., and Rubin, E. S. (2002). A technical, economic, and environmental assessment of amine-based CO₂ capture technology for power plant greenhouse gas control. *Environ. Sci. Technol.* 36, 4467–4475. doi: 10.1021/es0158861
- Rogers, R. D., and Seddon, K. R. (eds) (2003). *Ionic Liquids as Green Solvents: Progress and Prospects*. Washington, DC: American Chemical Society; ACS Symposium Series, 856.
- Sanna, A., Uibu, M., Caramanna, G., Kuusik, R., and Maroto-Valera, M. M. (2014). A review of mineral carbonation technologies to sequester CO₂. *Chem. Soc. Rev.* 43, 8049–8080. doi: 10.1039/C4CS00035H
- van Rantwijk, F., and Sheldon, R. A. (2007). Biocatalysis in ionic liquids. *Chem. Rev.* 107, 2757–2785. doi: 10.1021/cr050946x
- Wang, C. M., Luo, H. M., Jiang, D. E., Li, H. R., and Dai, S. (2010). Carbon dioxide capture by superbase-derived protic ionic liquids. *Angew. Chem. Int. Ed.* 49, 5978–5981. doi: 10.1002/anie.201002641
- Wang, C. M., Luo, H. M., Li, H. R., Zhu, X., Yu, B., and Dai, S. (2012). Tuning the physicochemical properties of diverse phenolic ionic liquids for equimolar CO₂ capture by the substituent on the anion. *Chem. Eur. J.* 18, 2153–2160. doi: 10.1002/chem.201103092
- Wang, C. M., Luo, X. Y., Luo, H. M., Jiang, D. E., Li, H. R., and Dai, S. (2011). Tuning the basicity of ionic liquids for equimolar CO₂ capture. *Angew. Chem. Int. Ed.* 50, 4918–4922. doi: 10.1002/anie.201008151
- Wang, N., Xu, J., and Lee, J. K. (2018). The importance of N-heterocyclic carbene basicity in organocatalysis. *Org. Biomol. Chem.* 16, 8230–8244. doi: 10.1039/C8OB01667D
- Wang, Z., Gao, F. X., Ji, P., and Cheng, J. P. (2018a). Unexpected solvation-stabilization of ions in a protic ionic liquid: insights disclosed by a bond energetic study. *Chem. Sci.* 9, 3538–3543. doi: 10.1039/C7SC05227H
- Wang, Z., Wang, F., Xue, X. S., and Ji, P. (2018b). Acidity scale of N-heterocyclic carbene precursors: can we predict the stability of NHC-CO₂ adducts? *Org. Lett.* 20, 6041–6045. doi: 10.1021/acs.orglett.8b02290
- Watanabe, M., Thomas, M. L., Zhang, S., Ueno, K., Yasuda, T., and Dokko, K. (2017). Application of ionic liquids to energy storage and conversion materials and devices. *Chem. Rev.* 117, 7190–7239. doi: 10.1021/acs.chemrev.6b00504
- Welton, T. (1999). Room-temperature ionic liquids. Solvents for synthesis and catalysis. *Chem. Rev.* 99, 2071–2084. doi: 10.1021/cr980032t
- Xia, S. M., Chen, K. H., Fu, H. C., and He, L. N. (2018). Ionic liquids catalysis for carbon dioxide conversion with nucleophiles. *Front. Chem.* 6:462. doi: 10.3389/fchem.2018.00462
- Yang, J. D., Ji, P., Xue, X. S., and Cheng, J. P. (2018). Recent advances and advisable applications of bond energetics in organic chemistry. *J. Am. Chem. Soc.* 140, 8611–8623. doi: 10.1021/jacs.8b04104
- Yang, Q., Wang, Z., Bao, Z., Zhang, Z., Yang, Y., Ren, Q., et al. (2016). New insights into CO₂ absorption mechanisms with amino-acid ionic liquids. *ChemSusChem* 9, 806–812. doi: 10.1002/cssc.201501691
- Yasuda, T., and Watanabe, M. (2013). Protic ionic liquids: fuel cell applications. *MRS Bull.* 38, 560–566. doi: 10.1557/mrs.2013.153
- Zhu, X., Song, M. L., and Xu, Y. J. (2017). DBU-based protic ionic liquids for CO₂ capture. *ACS Sustain. Chem. Eng.* 5, 8192–8198. doi: 10.1021/acssuschemeng.7b01839

Conflict of Interest Statement: The authors declare that the research was conducted in the absence of any commercial or financial relationships that could be construed as a potential conflict of interest.

Copyright © 2019 Gao, Wang, Ji and Cheng. This is an open-access article distributed under the terms of the Creative Commons Attribution License (CC BY). The use, distribution or reproduction in other forums is permitted, provided the original author(s) and the copyright owner(s) are credited and that the original publication in this journal is cited, in accordance with accepted academic practice. No use, distribution or reproduction is permitted which does not comply with these terms.